Acta Biochim Biophys Sin (2009): 792–799 | © The Author 2009. Published by ABBS Editorial Office in association with Oxford University Press on behalf of the Institute of Biochemistry and Cell Biology, Shanghai Institutes for Biological Sciences, Chinese Academy of Sciences. DOI: 10.1093/abbs/gmp068.
Advance Access Publication 30 July 2009

Anti-tumor activity and immunological modification of ribosome-inactivating protein (RIP) from *Momordica charantia* by covalent attachment of polyethylene glycol

Mengen Li[1], Yiwen Chen[1], Zhongyu Liu[1], Fubing Shen[2], Xiaoxiao Bian[1], and Yanfa Meng[1*]

[1]Key Laboratory of Bio-resources and Eco-environment Ministry of Education, College of Life Science of Sichuan University, Chengdu 610064, China
[2]Department of Laboratory Medicine, Chengdu Medical College, Chengdu 610083, China
*Correspondence address. Tel: +86-28-85471541; Fax: +86-28-85412571; E-mail: yfmeng0902@scu.edu.cn

Ribosome-inactivating proteins (RIPs) are a family of enzymes that depurinate rRNA and inhibit protein biosynthesis. Here we report the purification, apoptosis-inducing activity, and polyethylene glycol (PEG) modification of RIP from the bitter melon seeds. The protein has a homogenous N-terminal sequence of N-Asp-Val-Ser-Phe-Arg. Moreover, the RIP displayed strong apoptosis-inducing activity and suppressed cancer cell growth. This might be attributed to the activation of caspases-3. To make it available for *in vivo* application, the immunogenicity of RIP was reduced by chemical modification with 20 kDa $(mPEG)_2$-Lys-NHS. The inhibition activity of both PEGylated and non-PEGylated RIP against cancer cells was much stronger than against normal cells, and the antigenicity of PEGylated RIP was reduced significantly. Our results suggested that the PEGylated RIP might be potentially developed as anti-cancer drug.

Keywords apoptosis; bitter melon seed; PEGylation; ribosome-inactivating protein

Received: February 19, 2009 Accepted: May 8, 2009

Introduction

Ribosome inactivating proteins (RIPs) from angiosperm species [1–3], fungal species [2–5], and bacteria [2] are a family of RNA *N*-glycosidases, which inactivate ribosome through the site-specific deadenylation of the large ribosomal RNA [1,6], and the mechanism of cell entry and intracellular trafficking of certain types of RIPs has been well studied [7]. Recent studies demonstrated that RIPs also have anti-tumor and anti-viral properties [8]. For example, MAP30, a 30 kDa single-stranded RIP, was found to be able to inhibit HSV-2 and HSV-1 viral proliferation [9,10]. Interestingly, MAP30 also showed robust and broad anti-cancer activities against multiple cancer cells such as lymphoid leukemia, lymphoma, choriocarcinoma, melanoma, breast cancer, skin tumor, prostatic cancer, squamous carcinoma, human bladder carcinomas, and Hodgkin's disease [11–15]. The anti-cancer activities of RIPs are primarily attributed to apoptotic pathway. Based on these features, researchers are attempting to take advantage of the multi-functions of the RIP to develop RIP-based drugs for anti-viral infection and anti-cancers. However, the strong immunogenicity of RIPs has significantly limited their clinical applications.

Different approaches, such as site mutagenesis, protein chemistry and modification, have been employed to reduce the immunogenicity of RIPs. Among them, PEGylation has been found to be very effective [16]. The chemical attachment of polyethylene glycol (PEG) to therapeutic proteins led to several benefits: the extended plasma half-life, lower toxicity, and increased drug stability and solubility [16]. PEGylation also reduced antigenicity of foreign proteins and less likely trigger immune rejection in human. The Food and Drug Administration has approved the PEGylated forms of the therapeutic proteins such as adenosine deaminase, asparaginase, α-IFN, and a growth hormone antagonist [17].

In this study, we first purified the RIP from bitter melon seeds and then carried out PEG modification. PEGylation of the RIP (RIP-PEG) did not significantly affect its anti-tumor activity as measured by the caspase-3

assay, DNA fragmentation, and morphological analysis. Most importantly, the *in vivo* immunogenicity analysis indicated that RIP-PEG triggered much weaker immune response as indicated by 70% decrease of antigen-specific serum IgG levels. This work may facilitate future clinical investigations of bitter melon RIP.

Materials and Methods

Materials

Bitter melon seeds were obtained from the Institute of Agricultural Science and Technique of Sichuan Province, China. Human epidermal carcinoma A431 cells and immortalized human keratinocyte HaCaT cell lines were provided by West China Center of Medical Sciences of Sichuan University (Chengdu, China). Superdex 200, SP-Sepharose FF, and Superdex 75 were purchased from Amersham Pharmacia Biotech (Piscataway, USA). $(mPEG)_2$-Lys-NHS (20 kDa) was obtained from Shearwater Polymers (Huntsville, USA). BALB/c mice (female, 20 ± 2 g) purchased from the Laboratory Animal Center of Sichuan University were maintained according to the principles of the China Agricultural University Animal Care and Use Committee. They were housed in a room maintained at $23 \pm 2^{\circ}C$ with $50 \pm 10\%$ humidity and a 12 h light/12 h dark cycle (lights on from 8:00 a.m. to 8:00 p.m.). Food and water were provided *ad libitum* throughout the experiments. Food was withheld 12 h before blood collection. Complete Freund's adjuvant and incomplete Freund's adjuvant were obtained from Sigma-Aldrich (St. Louis, USA). Peroxidase-conjugated AffiniPure goat anti-mouse IgG was obtained from ZSGB-BIO (Beijing, China).

Purification of RIP from bitter melon seeds

Decorticated dried ripe bitter melon seeds were ground and homogenized in cold 50 mM HAC–NaAC buffer, pH 5.0. The slurry formed was stirred for 12 h at 4°C and then centrifuged at 15,000 *g* for 30 min at 4°C. After filtering through cheesecloth, the supernatant was fractionated by precipitation with ammonium sulfate (30–60%). The precipitate was dissolved and dialyzed against 50 mM sodium phosphate (pH 7.0) for 12 h at 4°C. The dialyzed sample was passed through a SP-Sepharose FF column equilibrated with the dialysis buffer. The retained protein was eluted with a linear gradient of 0–1 M NaCl in 50 mM sodium phosphate, pH 7.0, at a flow rate of 1 ml/min. The fractions were monitored by UV detector at 280 nm and analyzed by 12% SDS-PAGE. The fractions containing significant 30 kDa were collected and concentrated properly. The concentrated sample was further applied to a Superdex 75 column and eluted with 50 mM sodium phosphate (pH 7.0) containing 0.15 M NaCl, at a flow rate of 1.5 ml/min. The fractions containing ribosome inactivating protein, analyzed by 12% SDS-PAGE, were pooled, concentrated and then dialyzed against 50 mM sodium phosphate, pH 7.0. After passing through a 0.22-μm filter, the concentrated ribosome inactivating protein was stored at 4°C before use. Protein concentration was determined with the method of Lowry *et al*. [18], using bovine serum albumin as the standard.

Chemical synthesis of RIP-PEG conjugate

Fifty micrograms of PEG powder was added to 2.5 ml of 2 mg/ml RIP in 0.05 M borate buffer (pH 8.5) and was quickly mixed with gentle stirring at 4°C for 30 min. Reactive products were applied to a Superdex 200 column, which was previously equilibrated with 50 mM phosphate buffer (pH 7.0) containing 0.15 M NaCl, and then column was eluted with the same equilibrium buffer at 1.5 ml/min of flow rate. The fractions were monitored by UV detector at 280 nm and pooled and then analyzed by 12% SDS-PAGE. Fractions with the RIP-PEG conjugate was collected and concentrated and then dialyzed against 50 mM phosphate buffer (pH 7.0). The RIP-PEG conjugate at 10 mg/ml was filtered through 0.22-μm membrane and stored at 4°C until use.

Cell culture

Cells were maintained in Dulbecco's modified Eagle's medium (DMEM) (Gibco BRL, Grand Island, USA) supplemented with 10% heat-inactivated fetal bovine serum (FBS) (Gibco BRL), 100 μg/ml penicillin and 100 U/ml streptomycin in a 5% CO_2 incubator (Thermo Forma 3110, Waltham, USA).

Measurement of cell growth inhibition by MTT assay

The MTT assay was used to evaluate the cytotoxicity of the RIP or RIP-PEG conjugate in human epidermal carcinoma A431 cells and immortalized human keratinocyte HaCaT cells. The stock solution of MTT [3-(4,5-dimethylthiozol-2-yl)-3,5-dipheryl tetrazolium bromide] (Sigma) was prepared using sterilized phosphate-buffered saline (PBS) of 5 mg/ml. The cells were suspended in DMEM supplemented with 10% fetal calf serum (pH 7.0–7.2), and seeded in 96-well plates (2×10^4 cells/well) and incubated at 37°C for 7 h in the incubator with 5% CO_2. Then, these cells were exposed to the RIP or RIP-PEG conjugate at 33, 3.3, 0.33, or 0.033 μM for 96 h. For A431 cells, 3.3 μM RIP or RIP-PEG conjugate was added followed by 48, 72 and

96 h incubation. Each concentration was tested in quadruplicate. At the end of the treatment, the cells were photographed under phase contrast microscope (TH4-200, Olympus, Tokyo, Japan). The 20 μl (5 mg/ml) of MTT was then added to each well and the plates were incubated at 37°C for 4 h. To each well 100 μl of acidified isobutyl alcohol (0.04 M HCl in isopropanol) was added. The OD of each well was read by a microplate spectrophotometer (Model 680, Bio-RAD, Hercules, USA) equipped with 570 nm filter. Cells without the RIP or RIP-PEG conjugate were used as control. The percentage of inhibition was calculated by the following formula, and experiments were repeated three times.

$$\text{Inhibition } (\%) = \frac{\text{OD}_{570\text{control}} - \text{OD}_{570\text{sample}}}{\text{OD}_{570\text{control}}} \times 100\%$$

Caspase-3 activity assay

The activity of caspase-3 was determined using the caspase-3 activity kit (Beyotime Institute of Biotechnology, Nantong, China). To evaluate the activity of caspase-3, A431 cells were treated with the 3.3 μM RIP or RIP-PEG conjugate, the cell lysates were respectively collected at 0, 12, 24, 36 h after exposure. After incubating the mixture composed of 10 μl of cell lysate, 80 μl of reaction buffer [1% NP-40, 20 mM Tris–HCl (pH 7.5), 137 mM NAD, and 10% glycerol] and 10 μl of 2 mM caspase-3 substrate (Ac-DEVD-pNA) in 96-well microtiter plates at 37°C for 4 h, samples were measured using the microplate spectrophotometer at 405 nm. The caspase activities were measured as fold of enzyme activity in comparison with control. All the experiments were carried out three times.

Hoechst 33258 staining

Apoptotic morphological changes in the nuclear chromatin of A431 cells were detected by Hoechst 33258 staining using the apoptotic nuclear chromatin staining kit (Applygen Technologies Inc., Beijing, China). A431 cells were incubated in DMEM with 10% FBS in 50-ml flask. Twenty-four hours later, cells were treated with the 3.3-μM RIP or RIP-PEG conjugate. Cells incubated in the absence of the RIP or RIP-PEG were used as control. After incubation for 48 h, cells were collected by centrifuging for 5 min at 1000 rpm and washed with PBS and then fixed with 4% paraformaldehyde for 10 min, and incubated with 50 μM Hoechst33258 staining solution for 10 min. After three washes with PBS, the cells were observed by a fluorescence microscope (TH4-200, Olympus).

DNA fragmentation analysis

After exposure to different concentrations of the RIP or RIP-PEG conjugate (0, 3.3 μM) for 48 h, A431 cells (1×10^6 cells) were collected and rinsed with cold PBS. Fragmented DNA was isolated by apoptotic DNA ladder kit (Applygen Technologies Inc.) according to the manufacturer's instructions. The eluate containing DNA pellets were electrophoresed on a 1.0% agarose gel at 45 V for 3 h. The gel was examined and photographed by an ultraviolet gel documentation system (Bio-RAD).

Flow cytometric analysis

Cellular DNA content and cell distribution were quantified by flow cytometry using propidium iodide (PI). After treatment with the RIP or RIP-PEG conjugate (3.3 μM) for 48 h, cells were collected and washed in ice-cold PBS and fixed with 70% ethanol. The fixed cells were harvested by centrifugation at 1000 rpm for 5 min and dissolved in 1 ml PBS containing 50 μg/ml RNase A, 50 μg/ml PI, 0.1% Triton X-100, and 0.1 mM EDTA (pH 7.4), and incubated at 37°C for 30 min. The fluorescence was measured by flow cytometry (ELITE ESP, Coulter, Fullerton, USA).

Immunogenicity analysis

BALB/C mice were randomly classified into control, RIP, and RIP-PEG conjugate groups with 10 mice in each group. The mice were injected subcutaneously with the RIP or RIP-PEG conjugate emulsified in Freund's complete adjuvant in four limbs at the dose of 2 mg/kg. Two weeks and 4 weeks after the first injection, two booster injections of the RIP or RIP-PEG conjugate emulsified in Freund's incomplete adjuvant were given to each mouse. Two weeks after the booster injection, blood samples were collected from the capillary vessel in mice's eyes. Separated sera were prepared and stored at −20°C.

Antigen-specific serum IgG levels were measured by ELISA. Briefly, 96-well plates were coated with 100 μl of 3 μg/ml purified antigen (RIP) in 0.1 M carbonate-coating buffer, pH 9.5, and incubated overnight at 4°C. After washing, 300 μl of PBS containing 10% FBS, pH 7.4, were added to each well followed by 2 h incubation at 37°C. Diluted sera (1:16) were added (100 μl/well) and followed by 2 h incubation at 37°C. Wells were then washed in PBS washing buffer, pH 7.4, containing 0.05% Tween-20, and then incubated with peroxidase-conjugated AffiniPure goat anti-mouse IgG (1:40,000) for 1 h at 37°C. Then, the plate was washed five times in PBST followed by the addition of 100 μl/well tetramethyl benzidine (Sigma) as a substrate for horseradish

peroxidase. The reactions were allowed to develop at 37°C for 15 min. Then, 50 μl of 2 M sulfuric acid was added to stop the reaction. The absorbance was measured with the microplate spectrophotometer at 450 nm.

Statistical analysis

All assays were conducted three times. Data are presented as mean ± SD. The Duncan test and one-way analysis of variance were used for multiple comparisons (SPSS version 13.0, SPSS, Chicago, USA).

Results

PEGylation of RIP from bitter melon seeds

As examined by SDS-PAGE, PAGE, gradient PAGE and TSK 3000 column, pure bitter melon RIP was obtained through extraction and chromatography with SP-Sepharose FF and Superdex 75. RIP is an alkaline glycoprotein consisting of a single polypeptide chain with a molecular mass of 30 kDa and a pI of 9.0. Protein sequencing indicated a homogenous N-terminal with a sequence of N-Asp-Val-Ser-Phe-Arg.

Modified products of RIP with PEG polymer were separated on Superdex 200 molecular sieve column and analyzed by SDS-PAGE. The results showed that modified products were free RIP and RIP-PEG conjugate. The molecular weight of the targeted RIP-PEG conjugate is within 70–110 kDa by SDS-PAGE in non-reducing conditions, indicating that 2–4 of PEG molecules were conjugated on each RIP molecule (**Fig. 1**). The purity and molecular weight of the RIP-PEG conjugate were also analyzed by HPLC (**Fig. 2**).

Effects of RIP and RIP-PEG conjugate on the proliferation of A431 and HaCaT cells

As Fig. 3 showed, both the RIP and RIP-PEG conjugate exhibited dose- and time-dependent inhibition to the growth of human epidermal carcinoma A431 cells. Under the same concentration, PEGylation of RIP allowed to some extent decrease, approximately 20%, compared with the native RIP in A431 cells [**Fig. 3(A,B)**]. However, cell growth inhibition of the RIP and RIP-PEG conjugate to HaCaT cells demonstrated a significant decrease to A431 cells, indicating that both the RIP and RIP-PEG conjugate displayed stronger inhibition against cancer cells than against normal cells [**Fig. 3(C)**].

Under a phase contrast microscope, untreated A431 cells displayed extended and flat cell shape. After exposure to 33 μM of the RIP or RIP-PEG conjugate for 96 h, A431 cells showed typical apoptotic morphological changes such as blebbing, loss of membrane asymmetry,

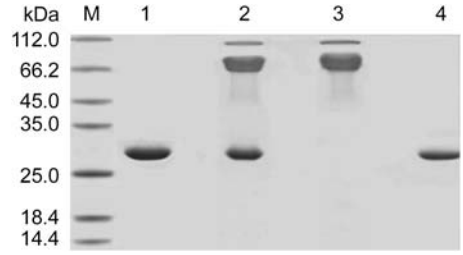

Figure 1 SDS-PAGE of RIP-PEG conjugate isolated by Superdex 200 molecular sieve column M, molecular mass protein markers; lane 1, RIP as control; lane 2, mixture of RIP and RIP-PEG conjugate; lane 3, RIP-PEG conjugate; and lane 4, non-modified RIP.

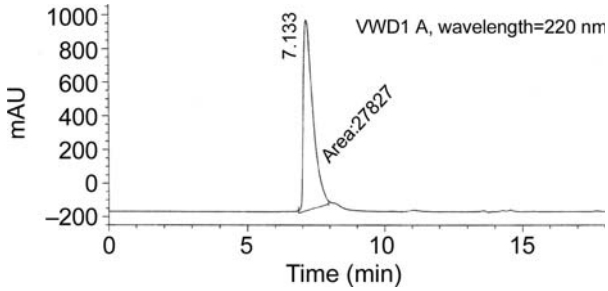

Figure 2 Profile of RIP-PEG conjugate by HPLC Analysis conditions: TOSOH TSK-GEL G2000SWxl (7.8 × 300); buffer, 0.2 M Na_2SO_4, 50 mM Tris–HCl, pH 7.3; flow rate, 0.8 ml/min; detection wavelength, 220 nm.

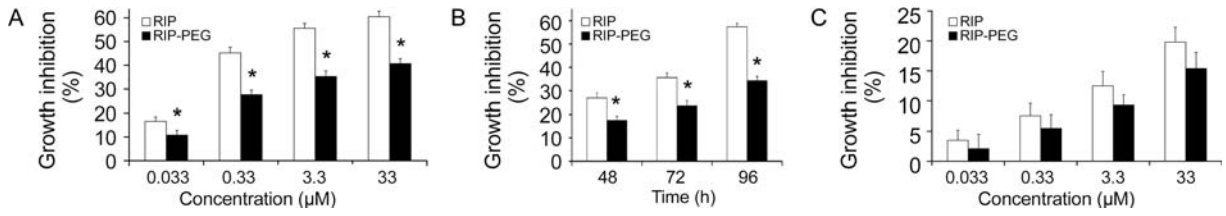

Figure 3 Inhibition effects of RIP or RIP-PEG conjugate on the proliferation of human epidermal carcinoma A431 cells and immortalized human keratinocyte HaCaT cells (A) Dose-dependent inhibition of the proliferation of human epidermal carcinoma A431 by RIP or RIP-PEG conjugate at different concentrations. (B) Time-dependent effects of the 3.3 μM RIP or RIP-PEG conjugate on the inhibition of human epidermal carcinoma A431. (C) Dose-dependent inhibition of the proliferation of immortalized human keratinocyte HaCaT cells by RIP or RIP-PEG conjugate at different concentrations. Value represents the mean ± SD of three independent experiments. *$P < 0.05$ compared with RIP.

cell shrinkage, etc. [**Fig. 4(A–C)**]. In contrast, the majority of either the treated or untreated HaCaT cells displayed normal morphological performance [**Fig. 4(D–F)**].

Caspase-3 activity

As an execution caspase, caspase-3 plays a pivotal role in apoptotic initiation. As shown in **Fig. 5**, the 3.3 μM RIP or RIP-PEG conjugate treatment triggered time-dependent increase in caspase-3 activity, which was first detected at 12 h, reached peak at 24 h. The activity was maintained until 36 h after treatment.

Nuclear morphological changes

As **Fig. 6** showed, under fluorescence microscope, untreated A431 cells displayed extended and flat cell bodies with uniform chromatin across the nuclei, whereas treated cells by RIP or RIP-PEG conjugate showed nuclear morphological changes with apoptotic

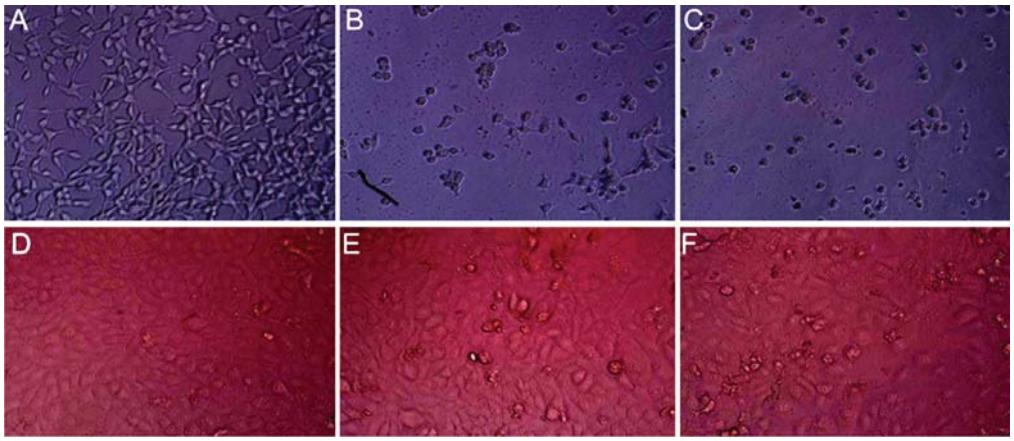

Figure 4 Phase contrast microscope photos of cytotoxicity assay of RIP or RIP-PEG conjugate for 96 h (200×) (A) Normal control of human epidermal carcinoma A431 cells. (B) Human epidermal carcinoma A431 cells treated with 33 μM RIP-PEG conjugate. (C) Human epidermal carcinoma A431 cells treated with 33 μM RIP. (D) Normal control of immortalized human keratinocyte HaCaT cells. (E) Immortalized human keratinocyte HaCaT cells treated with 33 μM RIP-PEG conjugate. (F) Immortalized human keratinocyte HaCaT cells treated with 33 μM RIP.

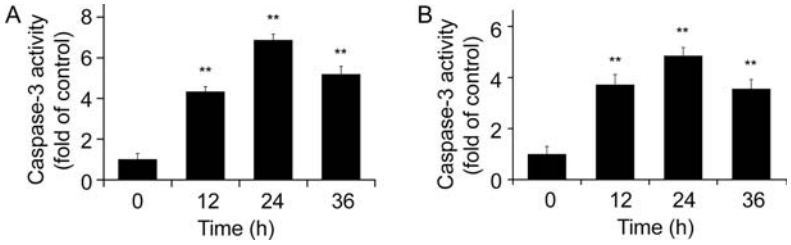

Figure 5 Activation of caspase-3 (A) RIP-induced caspase-3 activation in A431 cells. (B) RIP-PEG conjugate-induced caspase-3 activation in A431 cells. The cells were incubated with the 3.3 μM RIP or RIP-PEG conjugate for 0, 12, 24, 36 h. Data are the mean ± SD of three independent experiments. $^{**}P < 0.01$ compared with control group (0 h). The value of control was set to 1.

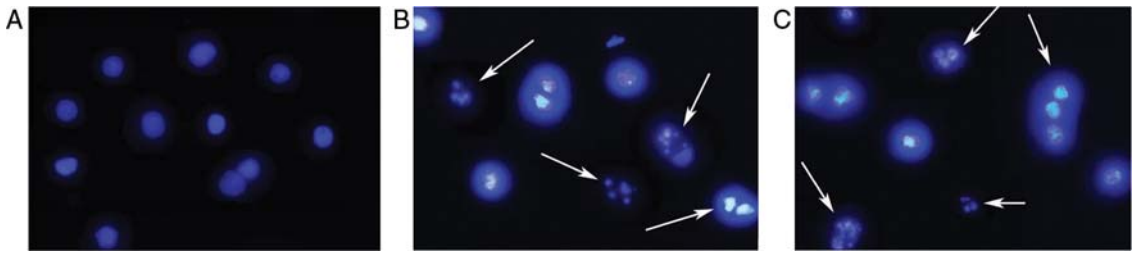

Figure 6 Morphological analysis of RIP or RIP-PEG conjugate-treated A431 cells apoptosis by Hoechst 33258 staining (600×) (A) In controls, the majority of cells had uniformly stained nuclei. (B) After exposure to the 3.3 μM RIP-PEG conjugate for 48 h, A431 cells showed typical morphological changes of apoptosis (nuclei fragmentation with condensed chromatin). (C) Cells treated with the 3.3 μM RIP for 48 h also showed morphological changes of apoptosis.

characteristics, such as nuclei condensation, boundary aggregation or split and nucleus fragmentation.

DNA fragmentation

After the A431 cells were exposed to the 3.3-μM RIP or RIP-PEG conjugate for 48 h, typical DNA laddering was observed (**Fig. 7**). In contrast, no DNA laddering was observed in untreated A431 cells. Thus, DNA laddering further confirmed that RIP or RIP-PEG conjugate could induce apoptosis in A431 cells.

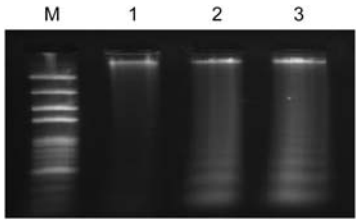

Figure 7 DNA laddering induced after exposure to the 3.3 μM RIP and RIP-PEG conjugate in the cultured A431 cells for 48 h measured on agarose gel electrophoresis M, DNA ladder mark; lane 1, untreated A431 cells; lane 2, 3.3 μM RIP-PEG conjugate treatment for 48 h; and lane 3, 3.3 μM RIP treatment for 48 h.

Detection of apoptotic A431 cells induced by RIP and RIP-PEG conjugate

To further measure the apoptotic induction activity of the RIP and RIP-PEG conjugate, A431 cells were stained with PI, and the sub-G_1 cell population was examined by flow cytometry. After treatment with the 3.3-μM RIP or RIP-PEG conjugate for 48 h, massive cell death was observed as indicated by the emerging of large amount of sub-G_1 population. This treatment also resulted in accumulation of cells in the G_1 phase and reduction of cells in the S phase along with blockage of cell proliferation (**Fig. 8**). The G_1 phase arrest eventually led to cell deaths at protracted incubation with the 3.3-μM RIP or RIP-PEG conjugate. Cell cycle analysis indicated that treatment with the RIP or RIP-PEG conjugate decreased the proportion of cells in the S phase and increased the proportion of cells in the G_0/G_1 and G_2/M phases of cell cycle. In untreated A431 cells, the mean apoptotic population was 5.0%, which increased to 46.7% and 27.0% after treatment with the 3.3 μM RIP and RIP-PEG conjugate for 48 h, respectively (**Fig. 8**). The number of G_0/G_1 phases of apoptotic A431 cells increased from 45.0% to 81.1% and 55.7% after 48 h of exposure to the 3.3 μM RIP or RIP-PEG conjugate, the

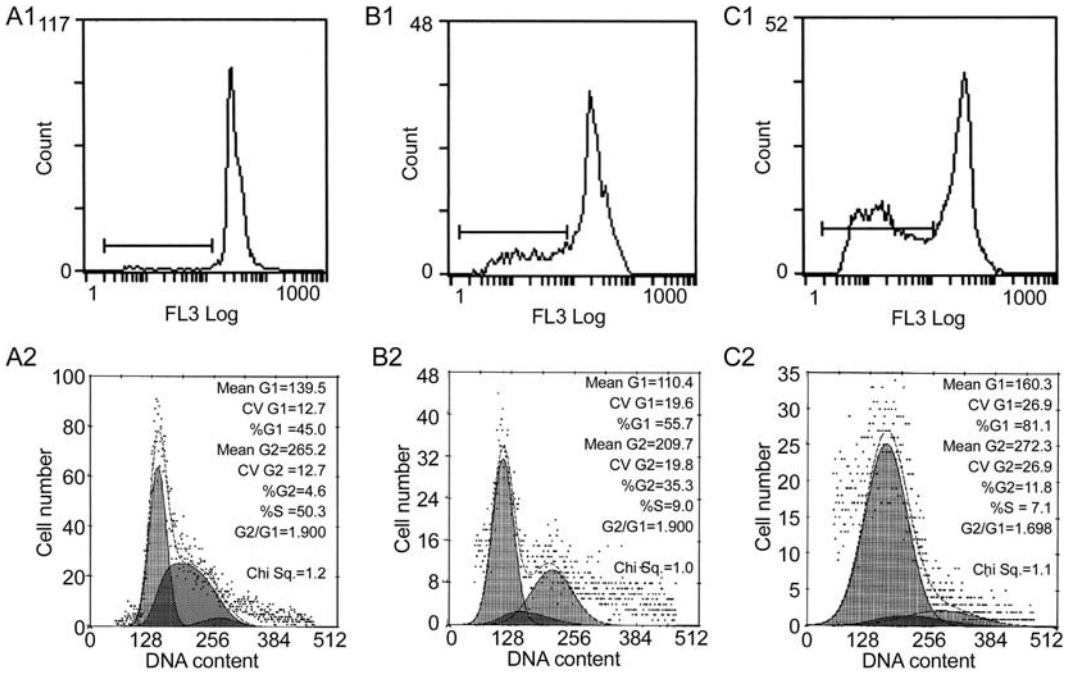

Figure 8 Flow cytometry analysis of the A431 cells affected by the RIP or RIP-PEG conjugate (A1) Histogram of the genomic DNA of the untreated A431 cells. (B1) Histogram of the genomic DNA of the A431 cells incubated with the 3.3 μM RIP-PEG conjugate for 48 h. (C1) Histogram of the genomic DNA of the A431 cells incubated with the 3.3 μM RIP for 48 h. (A2) Analysis of the cell cycle of the untreated A431 cells. (B2) Analysis of the cell cycle of the A431 cells incubated with the 3.3 μM RIP-PEG conjugate for 48 h. (C2) Analysis of the cell cycle of the A431 cells incubated with the 3.3 μM RIP for 48 h. After treated with RIP or RIP-PEG conjugate cells cycle distribution changed, the proportion of G_0/G_1 phases and G_2/M phases increased significantly ($P < 0.05$) and the proportion of the S phase decreased significantly ($P < 0.05$).

G_2/M phase increased from 4.6% to 11.8% and 35.3%, whereas the S phase decreased from 50.3% to 7.1% and 9.0%, respectively (**Fig. 8**).

Immunogenicity analysis of RIP-PEG conjugate and RIP *in vivo*

The antigenicity of RIP and RIP-PEG conjugate was evaluated by measuring the specific IgG antibody titers of the serum of the BALB/c mice immunized with RIP or RIP-PEG conjugate. As shown in **Fig. 9**, the serum obtained from the mice immunized with RIP-PEG conjugate produced IgG antibody titer was lower than the antibody titer produced using RIP.

Discussion

Apoptosis, a programmed process of cell death controlled at the gene level, has been considered a 'final common pathway of cell suicide'. It plays important roles in embryonic development, tissue homeostasis maintenance, and elimination of stray and DNA-damaged cells [19,20]. Histologically, apoptotic cells are characterized by morphological alterations such as cell shrinkage, nuclear chromatin compaction, pyknosis, nuclear fragmentation, cytoplasmic condensation, and convolution of the nuclear and cell outlines [21]. Our results showed that the RIP or RIP-PEG conjugate induced apoptosis and suppressed A431 cell proliferation in a time- and dose-dependent manner. Under the same concentration, the inhibition rate of RIP-PEG conjugate for A431 is about 60% of RIP. But both the RIP and RIP-PEG conjugate showed little toxic to immortalized human keratinocyte HaCaT cells. Because of the steric effect of surface tethered hydrophilic PEG chains on receptor bindings of cells or protein–protein interactions or PEG molecules may overlay the surface of the RIP, the partial active sites of the RIP were blocked, and the PEGylated proteins exhibited the slight loss of biologic activities *in vitro*.

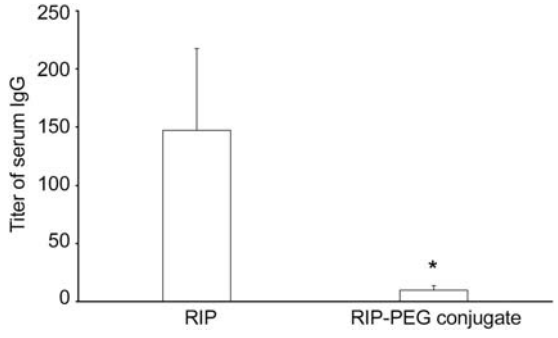

Figure 9 The specific IgG antibody titer of mice immunized with RIP or RIP-PEG conjugate The specific IgG antibody titers of the serum of the BALB/c mice immunized with RIP or RIP-PEG conjugate were determined using ELISA as described in 'Materials and Methods'. The specific IgG antibody titers of RIP-PEG conjugate decreased significantly compared with that of RIP ($P < 0.05$).

Cysteine aspartases (caspases), a protease family, are known to be required for apoptosis induced by various stimuli [22]. Among mammalian caspases, comprising at least 14 known members, caspase-3 is thought to be the main effecter of caspases and has been identified as being activated in response to cytotoxic drugs [22]. Activation of caspase-3 is an important step in the execution phase of apoptosis and its inhibition blocks cell apoptosis [23]. In mammals, caspase-3 has been identified as key executors of apoptosis and is one of the most important caspases activated downstream of apoptotic pathways [24], which activates caspase-activated DNase, causing apoptotic DNA fragmentation. In order to determine whether RIP and RIP-PEG conjugate could induce apoptosis via caspase pathway, we examined caspase-3 activities and DNA fragmentations. We found that caspase-3 activation persisted in a time-dependent manner when exposed to RIP and RIP-PEG conjugate. The occurrence of DNA laddering in the exposed cells further confirmed the apoptotic-inducing activity of RIP.

Our data demonstrated that RIP and RIP-PEG conjugate have a high capacity of suppressing cell proliferation and triggering apoptosis of human epidermal carcinoma A431 cells in a time- and dose-dependent manner. Therefore, it may have therapeutic potential as an anticancer drug candidate. We also found that RIP and RIP-PEG conjugate can induce accumulation of cells arrested at G_1 phases of the cell cycle and cell apoptosis which may result in multiple mechanisms of action. It appears that the terminal stage apoptotic cells and necrotic cells were predominant 48 h later, which was more significant in the 3.3 μM RIP-treated group. Hence, it suggested that the inhibitory effect of RIP and RIP-PEG conjugate on A431 cells was mediated through the apoptotic pathway.

Immunogenicity of antigen has been the major barrier for *in vivo* application of protein therapeutic agents. In this study, we used the anti-serum IgG levels to estimate the immunogenicity of antigens in the animals. Results showed that the immunogenicity of the RIP-PEG conjugate was reduced significantly. This result is similar to PEG-methioninase, another PEGylated anti-cancer enzyme [25]. The PEGylated methioninase conjugate

also demonstrated an increased pharmacokinetic efficacy by increasing plasma half-life *in vivo*. Future studies of the RIP-PEG conjugate should involve pharmacokinetic investigations, since long-term retention of RIP depletion *in vivo* is very important to its future clinical applications.

In conclusion, we isolated and purified the RIP from bitter melon, and chemically modified the protein with PEG. Both the RIP and RIP-PEG conjugate showed a strong anti-tumor activity through apoptotic pathway, with less toxicity to normal cells. Moreover, the reduced antigenicity of the RIP *in vivo* was also achieved by the PEG modification of RIP. Thus, successful PEG modification of the RIP moved one step forward for its *in vivo* applications.

Funding

This work was supported by a grant from the National Natural Science Foundation of China (No. 30770232).

References

1 Stirpe F and Battelli MG. Ribosome-inactivating proteins: progress and problems. Cell Mol Life Sci 2006, 63: 1850–1866.
2 Girbés T, Ferreras JM, Arias FJ and Stirpe F. Description, distribution, activity and phylogenetic relationship of ribosome-inactivating proteins in plants, fungi and bacteria. Mini Rev Med Chem 2004, 4: 461–476.
3 Ruggieroa A, Chambery A, Di Maro A, Mastroianni A, Parente A and Berisio R. Crystallization and preliminary X-ray diffraction analysis of PD-L1, a highly glycosylated ribosome inactivating protein with DNase activity. Protein Pept Lett 2007, 14: 407–409.
4 Ng TB, Lam YW and Wang HX. Calcaelin, a new protein with translation-inhibiting, antiproliferative and antimitogenic activities from the mosaic puffball mushroom *Calvatia caelata*. Planta Med 2003, 69: 212–217.
5 Ng TB, Parkash A and Tso WW. Purification and characterization of alpha- and beta-benincasins, arginine/glutamate-rich peptides with translation-inhibiting activity from wax gourd seeds. Peptides 2003, 24: 11–16.
6 Endo Y and Tsurugi K. The RNA *N*-glycosidase activity of ricin A-chain: the characteristics of the enzymatic activity of ricin A-chain with ribosomes and with rRNA. J Biol Chem 1988, 263: 8735–8739.
7 Roberts L and Lord J. Ribosome-inactivating proteins: entry into mammalian cells and intracellular routing. Mini Rev Med Chem 2004, 4: 505–512.
8 Ng TB, Chan WY and Yeung HW. Proteins with abortifacient, ribosome inactivating, immunomodulatory, antitumor and anti-AIDS activities from Cucurbitaceae plants. Gen Pharmacol 1992, 23: 579–590.
9 Foa-Tomasi L, Campadelli-Fiume G, Barbieri L and Stirpe F. Effect of ribosome-inactivating proteins on virus-infected cells. Inhibition of virus multiplication and of protein synthesis. Arch Virol 1982, 71: 323–332.
10 Bourinbaiar AS and Lee-Huang S. The activity of plant-derived antiretroviral proteins MAP30 and GAP31 against herpes simplex virus *in vitro*. Biochem Biophys Res Commun 1996, 219: 923–929.
11 Ng TB, Liu WK, Sze SF and Yeung HW. Action of alphamomorcharin, a ribosome inactivating protein, on cultured tumor cell lines. Gen Pharmacol 1994, 25: 75–77.
12 Battelli MG, Polito L, Bolognesi A, Lafleur L, Fradet Y and Stirpe F. Toxicity of ribosome-inactivating proteins-containing immunotoxins to a human bladder carcinoma cell line. Int J Cancer 1996, 68: 485–490.
13 Ganguly C, De S and Das S. Prevention of carcinogen-induced mouse skin papilloma by whole fruit aqueous extract of *Momordica charantia*. Eur J Cancer Prev 2000, 9: 283–288.
14 Sun Y, Huang PL, Li JJ, Huang YQ, Zhang L, Huang PL and Lee-Huang S. Anti-HIV agent MAP30 modulates the expression profile of viral and cellular genes for proliferation and apoptosis in AIDS-related lymphoma cells infected with Kaposi's sarcoma associated virus. Biochem Biophys Res Commun 2001, 287: 983–994.
15 Basch E, Gabardi S and Ulbricht C. Bitter melon (*Momordica charantia*): a review of efficacy and safety. Am J Health Syst Pharm 2003, 65: 356–359.
16 Kozlowski A and Harris JM. Improvements in protein PEGylation: pegylated interferons for treatment of hepatitis C. J Control Release 2001, 72: 217–224.
17 Aguayo A, Cortes J, Thomas D, Pierce S, Keating M and Kantarjian H. Combination therapy with methotrexate, vincristine, polyethyleneglycol conjugated asparaginase, and prednisone in the treatment of patients with refractory or recurrent acute lymphoblastic leukemia. Cancer 1999, 86: 1203–1209.
18 Lowry OH, Roenbrough NJ, Farr AL and Randall RJ. Protein measurement with folin–phenol reagent. J Biol Chem 1951, 193: 265–275.
19 Kerr JF, Winterford CM and Harmon BV. Apoptosis. Its significance in cancer and cancer therapy. Cancer 1994, 73: 2013–2026.
20 Hale AJ, Smith CA, Sutherland LC, Stoneman VE, Longthorne VL, Culhane AC and Williams GT. Apoptosis: molecular regulation of cell death. Eur J Biochem 1996, 236: 1–26.
21 Toshihiko T, Horiuchi A, Ichikawa N, Mori A, Nikaido T and Fujii S. Inverse relationship between apoptosis and Bcl-2 expression in syncytiotrophoblast and fibrin-type fibrinoid in early gestation. Mol Hum Reprod 1999, 5: 246–251.
22 Krepela E. Cysteine proteinases in tumor cell growth and apoptosis. Neoplasma 2001, 48: 332–349.
23 Budihardjo I, Oliver H, Lutter M, Luo X and Wang X. Biochemical pathways of caspase activation during apoptosis. Annu Rev Cell Dev Biol 1999, 15: 269–290.
24 Cohen GM. Caspases: the executioners of apoptosis. Biochem J 1997, 326: 1–16.
25 Sun X, Yang Z, Li S, Tan Y, Zhang N, Wang X and Yagi S, *et al*. *In vivo* efficacy of recombinant methioninase is enhanced by the combination of polyethylene glycol conjugation and pyridoxal 5′-phosphate supplementation. Cancer Res 2003, 63: 8377–8383.